

Effect of formaldehyde gas adsorption on the electrical conductivity of Pd-doped TiO₂ thin films

A. Yildiz · D. Crisan · N. Dragan · N. Iftimie ·
D. Florea · D. Mardare

Received: 9 January 2011 / Accepted: 16 February 2011 / Published online: 26 February 2011
© Springer Science+Business Media, LLC 2011

Abstract 0.5 wt% Pd-doped titanium oxide thin films were obtained by dip-coating on silicon substrates. The films were compacted by annealing in air at 300 and 500 °C. Temperature dependent electrical conductivity measurements were performed in the temperature range 373–623 K, in different environments (air, methane, acetone, ethanol, formaldehyde and liquefied petroleum gas), to test the films sensing gas properties. Formaldehyde was found to be the test gas that produces the most significant changes in the electrical conductivity of the studied films. This was the reason why it was chosen to investigate its effect on their electrical conductivity. A model was proposed, the model of the potential fluctuations at grain boundaries. A comparison between some parameters obtained in the proposed model was performed as a function of annealing temperature, and as a function of gas atmosphere. The values of the mean barrier height and the standard deviation were estimated to range between 0.336–0.588 eV and 0.175–0.199 eV, respectively. It was found that formaldehyde leads to a rather sharp decrease in

the values of the barrier height and the standard deviation, and to an increase in the conductivity. We have observed the best sensing gas performance for the films annealed at 300 °C, comparing to their counterparts annealed at 500 °C, explained by the lowest values of the barrier energy height and the standard deviation.

1 Introduction

Formaldehyde is a volatile organic compound that can naturally occur in our environment during normal metabolic processes, being composed of carbon, hydrogen, and oxygen (chemical formula: HCHO). This compound can also appear in the environment as a product of combustion [1]. Because of its versatility, formaldehyde is an important industrial chemical material used to make household products, building materials, etc. It is mostly used in adhesives for wood products, being one of the more common indoor air pollutants [2]. It is reported to be toxic, allergenic and carcinogenic [3, 4]. Prolonged exposure to formaldehyde can lead to different symptoms like eye irritation, headaches, fatigue, respiratory problems, etc. Therefore, effective ways for the detection of such hazardous pollutants are required. An inexpensive, and relatively easy method, is to use an exposed metal oxide semiconducting film, and convert the chemical gas concentration directly into an electrical output, by measuring its electrical resistance [4, 5]. Films like TiO₂, or SnO₂, are most suited as gas sensors due to their desired sensitivity, and to their good mechanical and chemical stability in adverse environments [6]. Doping with metal nanoparticles (Pd, Pt, etc.) is an effective way to enhance the response magnitude [7–9]. These impurities decrease the activation energy of the reaction occurring on the surface, raising the

A. Yildiz (✉)
Department of Physics, Faculty of Science and Arts,
Ahi Evran University, 40040 Kirsehir, Turkey
e-mail: yildizab@gmail.com

D. Crisan · N. Dragan
Institute of Physical Chemistry “Ilie Murgulescu”,
202 Splaiul Independenței, 060021 Bucharest, Romania

N. Iftimie
National Institute of Research and Development for Technical
Physics, 47 Mangeron Blvd., 700050 Iasi, Romania

D. Florea · D. Mardare
Faculty of Physics, Alexandru Ioan Cuza University,
11, Carol I Blvd., 700506 Iasi, Romania

adsorption activity of the material [7–9]. Understanding the electrical transport properties of TiO₂ thin films is a prerequisite in the improvement of the sensitivity mechanism of gas sensors, but still remains the subject of an intensive discussion. Studies have been recently carried out by our team to determine the proper charge transport mechanisms in TiO₂ and SnO₂ thin films [10–16].

As pointed out in [17], polycrystalline TiO₂ is more suitable for gas sensing than TiO₂ as single crystal. In the polycrystalline materials, the electrical conductivity is determined by the potential barriers built up around grain boundaries. According to the grain boundary model, the grain boundary region consists in a large number of defects which act as effective carrier traps [18]. When these trapping states are occupied, they create a depletion region in the crystallite and a potential barrier at the interface [18]. To explain the gas sensing properties of polycrystalline TiO₂ films, it is mandatory to make a correlation between film's surface and grain boundary potential barriers. To the best of the authors' knowledge, there is no report available in the literature on the effect of formaldehyde gas adsorption on the electrical conductivity, by taking into account the grain boundary limited conduction model of Werner [19].

The aim of this work is to investigate the effect of formaldehyde gas adsorption on the electrical conductivity of the sol–gel Pd-doped TiO₂ films, deposited on silicon substrates, and heat-treated at different temperatures.

2 Experimental

Pd-doped TiO₂ films (0.5 wt% Pd) were deposited on silicon substrates (covered by a 510 nm oxide layer), by using the alkoxide route of the sol–gel method. First, the doped gels were obtained by simultaneous gelation of both precursors (for TiO₂ and Pd) in the sol–gel process. The titania source was the tetraethyl orthotitanate (95%, Merck), Ti(OC₂H₅)₄, while the source of palladium was Pd acetylacetonate (99%, Merck), C₁₀H₁₄O₄Pd. The solvent used for the both TiO₂ and Pd precursors was the absolute ethanol (min. 99.8 vol.%). The hydrolysis reaction took place in the presence of the water, in nitrogen atmosphere, under vigorous stirring. Doped TiO₂ gels, containing 0.5 wt% Pd related to TiO₂, were prepared. More experimental details, referring to the composition of the starting solutions, are presented in [20]. The un-supported porous materials, resulted from the gelling of the starting solutions at room temperature, were dried at 80 °C, and then thermally-treated in air, for 1 h, at 300 and 500 °C. Supported TiO₂-based vitreous films (mono and bi-layers) were obtained, by the dip-coating method, on unheated Si (100)p substrates, and then compacted by thermally treatment in air at the same mentioned temperatures.

X-ray diffraction (XRD) measurements have been carried out both on gels and films, by using a Bruker-AXS D8 Advance diffractometer (CuK_α radiation, $\lambda = 1.540591 \text{ \AA}$). Thin films thicknesses are under 100 nm, as found out by using an ellipsometric method [20] (Table 1). The weight percentage of the anatase phase (W_A), and the average crystallite size for the both identified phases in gels (anatase and rutile) have been determined, with an X-RAY 5.0 program (see Table 1).

To measure the thin films electrical resistances, silver electrodes (parallel one to each other at a distance of 0.8 mm) have been deposited on the films' surface, by thermal vacuum evaporation. The samples under study were first subjected to two successive heating/cooling cycles in air, within the temperature range 373–623 K. After that, the temperature dependence of the electrical conductivities became reversible indicating, in our opinion, the stabilization of the films structure and composition in the respective temperature range [21]. The temperature dependent electrical conductivity of the TiO₂ films was investigated in ambient air, and in formaldehyde gas atmosphere, in the temperature range 373–623 K.

To test the films gas sensing performance, the sample was mounted on a heater placed in a glass enclosure capable of controlling the different gas concentrations [5]. During the cooling process, the samples continued to be exposed to the formaldehyde gas. The gas sensitivity, $S = \frac{|R_a - R_g|}{R_a}$, was determined from the measured values of the electrical resistances in air (R_a) and in the formaldehyde gas atmosphere (R_g).

3 Results and discussion

X-Ray diffraction measurements performed on the studied films show an amorphous structure, while the XRD patterns from the un-supported gels resulted from the gelation of the starting solutions, used for the films preparation, show a polycrystalline structure (Fig. 1). We believe that the explanation is related to the film thickness which is around 70 nm, and the XRD pattern for the film is covered by that of the substrate. It has been experimentally established that the “shoulder” observed in Fig. 1a is due to the substrate. While the gels thermally-treated at 300 °C present only the anatase phase, rutile makes its presence (6 wt. %) in the gels thermally-treated at 500 °C. From Table 1, one can see that, by increasing the annealing temperature, T_a , from 300 to 500 °C, the average crystallite size almost double its value.

Our previous studies [5] done on the samples annealed at 500 °C (undoped and 0.5 wt% Pd-doped deposited on glass and Si substrates), regarding their sensitivity

Table 1 Annealing temperature (T_a), thickness (d), weight percentage of anatase phase (W_A), average crystallite size for the anatase phase (D_A) and for the rutile phase (D_R), electrical conductivity at the

T_a (°C)	d (nm)	W_A (%)	D_A (nm)	D_R (nm)	Air				Formaldehyde			
					σ_{513K} (Ωcm) ⁻¹	$\bar{\phi}$ (eV)	σ_ϕ (eV)	H	σ_{513K} (Ωcm) ⁻¹	$\bar{\phi}$ (eV)	σ_ϕ (eV)	H
300	71	100	18.5	0.0	5.55×10^{-11}	0.588 ± 0.015	0.199 ± 0.074	2.96	5.51×10^{-10}	0.336 ± 0.091	0.175 ± 0.058	1.92
500	72	94	30.7	29.5	5.23×10^{-11}	0.464 ± 0.012	0.187 ± 0.065	2.48	3.73×10^{-10}	0.386 ± 0.011	0.181 ± 0.061	2.15

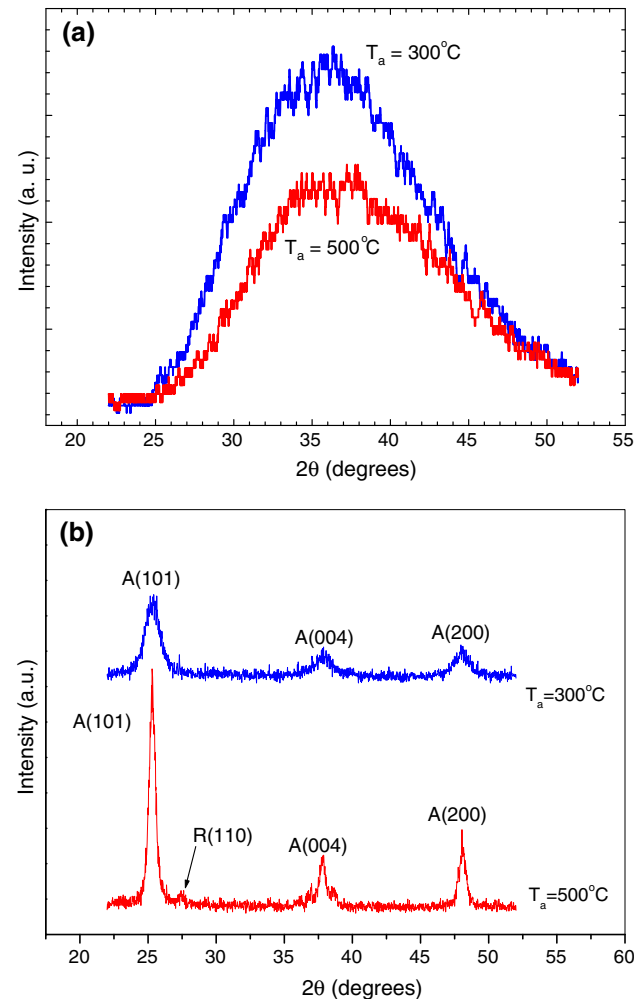


Fig. 1 XRD patterns of the studied films (a) and un-supported gels (b)

performances to five reducing test gases (liquefied petroleum gas (LPG), methane, acetone, ethanol and formaldehyde), revealed that, by Pd doping, titania films became very sensitive to formaldehyde, with a special remark for those deposited on silicon substrates. By performing now the same sensing gas tests, but for the Pd-doped films thermally treated at 300 °C (also deposited on Si), we have arrived to the same conclusion namely, formaldehyde,

optimum operating temperature (σ_{513K}), mean barrier height ($\bar{\phi}$), standard deviation (σ_ϕ), homogeneous coefficient (H), for films exposed to air and to formaldehyde

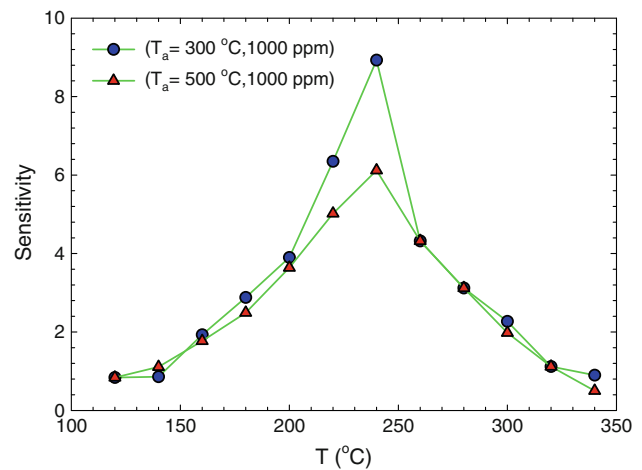


Fig. 2 The sensitivity of the studied samples in front of formaldehyde, plotted as a function of the operating temperature

followed by ethanol and acetone, is the test gas that produces the most significant changes in the electrical resistance of the studied films [5]. What was new here, was the enhancement in the sensitivity in front of all the test gases (especially in front of formaldehyde), with the decrease of the heat-treatment temperature. Figure 2 shows the sensitivity to formaldehyde at the optimum operating temperature (240 °C), for both thermally treated samples.

The best sensing properties of the studied films in front of formaldehyde, determined us to investigate its effect on their electrical conductivity. Figure 3 shows the dependences of the films electrical conductivity, σ , as a function of the inverse temperature, in the temperature range 373–623 K under different ambient conditions. We expect that these dependences obey the Arrhenius model—namely they exhibit linear dependencies, by plotting $\ln \sigma = f(10^3/T)$. In this model, the conductivity is expressed by:

$$\sigma = \sigma_0 \exp\left(-\frac{E_a}{k_B T}\right), \quad (1)$$

where σ_0 is a parameter depending on the semiconductor nature, E_a is thermal activation energy and k_B is the Boltzmann's constant. One can observe that the conductivity of all the films increases with the increase in the

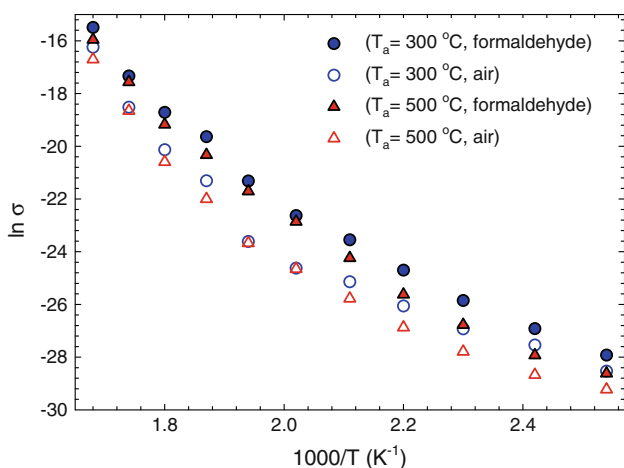
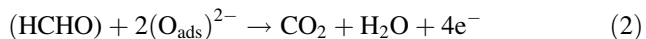


Fig. 3 Temperature dependence of the conductivity plotted as $\ln(\sigma)$ versus $10^3/T$ in the temperature range 373–623 K

temperature, but the experimental data, $\ln \sigma = f(10^3/T)$, can not be fitted by straight lines (the activation energy is not constant over the studied temperature domain); as a consequence, these dependencies do not obey the Arrhenius model.

From Table 1, it can be seen that the electrical conductivity (at the optimum operating temperature) slowly decreases with the increasing annealing temperature from 300 to 500 °C, while, by varying the ambient conditions, from air to formaldehyde, a sharp increase (about ten times) can be observed. Regarding the latter observation, an explanation could be related to the reaction between HCHO and the adsorbed oxygen [22], knowing that the oxygen species in the air are adsorbed on the films surface and ionized to O_{ads}^- and O_{ads}^{2-} :



The released electrons lead to the increase of the thin films electrical conductivity. This process results in the thinning of the depletion layer thickness.

In polycrystalline materials, the electrical transport mechanism is related to the grain boundaries. In our previous studies [12, 13], we have shown that the electrical conductivity obeys the classical grain boundary trapping theory [18]; according to this theory, in a polycrystalline film, the grain boundary region consists in a large number of defects which act as effective carrier traps [18]. When the trapping states in the grain boundary region are occupied, they create a depletion region in the crystallite and a potential barrier at the interface [18]. The presence of a large number of defects in the grain boundary region results in the formation of trapping states that are capable of trapping carriers. This reduces the number of free carriers available for electrical conduction. In the present study, Werner’s model [19] is introduced to interpret the

Arrhenius curved plots (see Fig. 3), and the fluctuations in the potential barrier height, together with the low homogeneity of the films, are made responsible for this behavior. According to this model, the electrical current density (J) across the grain boundaries is expressed as [19]:

$$J = A^* T^2 \exp(-q\xi/k_B T) \exp(-qV_{gb}/k_B T) [1 - \exp(-qV_d/k_B T)] \quad (3)$$

where A^* is the effective of Richardson constant, q is the electron charge, $q\xi$ is the Fermi level position within the grain: $q\xi = k_B T \ln(N_c/n)$, N_c is effective density of states, n is carrier density, V_{gb} is the barrier potential at the grain boundary, and V_d is the bias voltage. Assuming $V_{gb} \ll k_B T/q$, the grain boundary conductivity is obtained with the following relation,

$$\sigma = D \frac{dJ}{dV_{gb}} = \frac{DTqA^*}{k_B} \exp(-q\Phi/k_B T) \quad (4)$$

where D is the average crystallite size and $\Phi = V_{gb} + \xi$. Werner suggested the existence of the potential variations among different boundaries, and he modeled the fluctuating barriers Φ by a Gaussian probability distribution [19],

$$P(\phi) = \frac{1}{\sigma_\phi \sqrt{2\pi}} \exp\left[-\frac{(\bar{\phi} - \phi)^2}{2\sigma_\phi^2}\right]. \quad (5)$$

Here $\bar{\phi}$ denotes the mean barrier height (which limits the conduction of the carriers) and σ_ϕ is the standard deviation of the Gaussian distribution of the band bending, giving an evaluation of the errors on the barrier values. Integrating over all the possible barrier heights (Φ), the effective barrier height is obtained:

$$\Phi_{eff}(T) = \bar{\Phi}(T) - \frac{\sigma_\phi^2 q}{2k_B T} \quad (6)$$

The temperature dependent activation energy is given by,

$$W(T) = -k_B \frac{d}{dT} [\ln(\sigma/T)] = q \left[\bar{\Phi}(T) - \frac{\sigma_\phi^2 q}{k_B T} \right] \quad (7)$$

According to above equations, Werner has shown that the temperature dependence of the conductivity is well described by a parabola such as [19],

$$\ln(\sigma/T) = \frac{a}{T^2} - \frac{b}{T} - c, \quad (8)$$

where the parameters a , b and c do not depend on the temperature, being related to the mean barrier height, $\bar{\phi}$, and the standard deviation, σ_ϕ , by the following relations:

$$\sigma_\phi = \sqrt{\frac{2ak_B^2}{q^2}}, \quad (9)$$

$$\bar{\phi} = \frac{bk_B}{q} \quad (10)$$

As said before, the curvatures of the Arrhenius plots in Fig. 3 are relatively well described by taking into account a distribution of the barrier heights as suggested by the model of Werner [19]. Equation 8 is used to fit the experimental conductivity data in Fig. 4. One can see that the experimental data are well fitted by the parabola. From the fit, the values of a , b , and then the values of σ_ϕ and $\bar{\phi}$ are estimated (Table 1). The curves deduced from the derivative of the parabola are presented in Fig. 5. The dependences of the activation energy show a good linearity for all the investigated films (correlation coefficients higher than 0.99), indicating that the Werner's model is applicable in our case.

The well fits observed from Figs. 4 and 5 reveal that, for the studied domain of the temperature, the grain boundary scattering of the charge carriers dominates in the

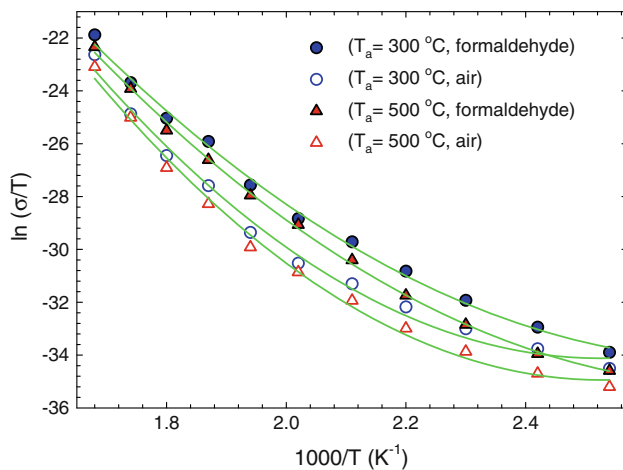


Fig. 4 Temperature dependence of the conductivity plotted as $\ln(\sigma/T)$ versus $10^3/T$. Solid lines are the best-fit lines with Eq. 8

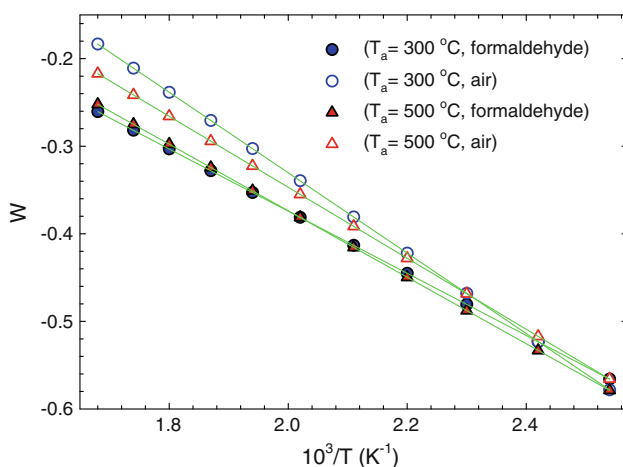


Fig. 5 The activation energy W versus $10^3/T$ for the studied thin films

investigated samples. On the other hand, the fittings are found to be better in the presence of formaldehyde. Both $\bar{\phi}$ and σ_ϕ increase with increasing annealing temperature. The presence of formaldehyde in environment leads to a rather sharp decrease in both parameters. The lowest values of these parameters are observed for the annealing temperature, $T_a = 300$ °C. In this case, $\bar{\phi}$ decreases in the presence of formaldehyde, from 0.588 to 0.336 eV, which explain its best sensing properties. In the studied samples, palladium impurities bring their own contribution in improving the gas sensitivity, since they give raise to the adsorption activity of the material.

Werner defines the homogeneous coefficient, H , as a ratio between the mean barrier height, $\bar{\phi}$, and the standard deviation, σ_ϕ [19]:

$$H = \bar{\phi}/\sigma_\phi. \quad (11)$$

This coefficient describes the film's homogeneity. Its values, reported in the literature for different materials, vary widely from 0.5 to 8 [23–25]. From Table 1, one can see that, the values of H , obtained for the investigated samples, are within this range, but its low values indicate that the films homogeneity is low. By exposing the films thermally-treated at 300 °C to formaldehyde, the homogeneous coefficient decreases from 2.96 to 1.92. This may indicate that, additional to grain boundary effects, a large number of other defects, such as oxygen vacancies, assumed to be also present in the studied films, could contribute to electrical conduction.

4 Conclusions

Pd-doped TiO_2 thin films (0.5 wt% Pd), obtained by the sol-gel method (dip-coating) on Si substrates and thermally-treated at 300 °C, exhibit better sensing properties than their counterparts thermally-treated at 500 °C, in front of five test gases (methane, acetone, ethanol, formaldehyde, LPG), with a special remark to formaldehyde. The best sensing properties of the studied films to formaldehyde, determined us to study its effect on their electrical conductivity. The temperature dependent electrical conductivity of the TiO_2 films was well described within the model of the potential fluctuations at grain boundaries, which gives the values of the mean barrier height—an important parameter in selecting a material for gas sensor. The presence of formaldehyde in the ambient was found to lead to a decrease in the values of the barrier height and the standard deviation, and to a sharp increase (about ten times) in the electrical conductivity. The lowest values of the barrier height and the standard deviation obtained for the films annealed at 300 °C, explain their best sensing gas performance.

Acknowledgments D. Mardare acknowledges the financial support from the grants PCCE-ID_76 and 12-128/2008.

References

1. Formaldehyde Epidemiology, Toxicology and Environmental Group, Formaldehyde and Facts About Health Effects (2002). http://www2.dupont.com/Plastics/en_US/assets/downloads/processing/FETEG_Facts.pdf
2. L. Feng, Y.J. Liu, X.D. Zhou, J.M. Hu, J. Colloid Interface Sci. **284**, 378 (2005)
3. O. Hernandez, L. Rhomberg, K. Hogan, C. Siegel-Scott, D. Lai, G. Grindstaff, M. Henry, J.A. Cotruvo, J. Hazard. Mater. **39**(2), 161 (1994)
4. J. Flueckiger, F.K. Ko, K.C. Cheung, Sensors **9**, 9196 (2009)
5. N. Iftimie, M. Crisan, A. Braileanu, D. Crisan, A. Nastuta, G.B. Rusu, P.D. Popa, D. Mardare, J. Optoelectron. Adv. M. **10**, 9–2363 (2008)
6. H. Tang, K. Prasad, R. Sanjinès, F. Lévy, Sensor Actuat. B **26–27**, 71 (1995)
7. F. Cosandey, G. Skandan, A. Singhal, JOM-e, **52**(10) (2000), <http://www.tms.org/pubs/journals/JOM/0010/Cosandey/Cosandey-0010.html>
8. W.K. Choi, S.K. Song, J.S. Cho, Y.S. Yoon, D. Choi, H.-J. Jung, S.K. Koh, Sensor Actuat. B **40**, 21 (1997)
9. N. Yamazoe, Sensor Actuat. B **5**, 7 (1991)
10. A. Yildiz, S.B. Lisesivdin, M. Kasap, D. Mardare, J. Non-Cryst. Solids **354**, 4944 (2008)
11. A. Yildiz, S.B. Lisesivdin, M. Kasap, D. Mardare, Physica B **404**, 1423 (2009)
12. A. Yildiz, S.B. Lisesivdin, M. Kasap, D. Mardare, J. Mater. Sci. Mater. Electron. **21**, 692 (2010)
13. A. Yildiz, N. Serin, M. Kasap, T. Serin, D. Mardare, J. Alloys Compd. **493**, 227 (2010)
14. T. Serin, A. Yildiz, N. Serin, N. Yıldırım, F. Özyurt, M. Kasap, J. Electron. Mater. **39**, 1152 (2010)
15. A. Yildiz, A.A. Alsaç, T. Serin, N. Serin, J. Electron. Mater. (2011). doi:10.1007/s10854-010-0228-2
16. A. Yildiz, F. Iacomi, D. Mardare, J. Appl. Phys **108**, 083701 (2010)
17. H.J. Höfler, H. Hahn, R.S. Averbach, Defect Diffus. Forum **75**, 195 (1991)
18. J.Y.W. Seto, J. Appl. Phys **46**, 5247 (1975)
19. J.H. Werner, Solid State Phenom. **37**, 213 (1994)
20. D. Crisan, N. Dragan, M. Crisan, M. Raileanu, A. Braileanu, M. Anastasescu, A. Ianculescu, D. Mardare, D. Luca, V. Marinescu, A. Moldovan, J. Phys. Chem. Solids **69**, 2548 (2008)
21. D. Mardare, G.I. Rusu, J. Non-Cryst. Solids **28–30**, 1395 (2010)
22. T. Wolkenstein, *Electronic Process on Semiconductor Surfaces During Chemisorption* (Consultats Bureau, New York, 1991)
23. S. Seeger, R. Mientus, J. Röhrich, E. Strub, W. Bohne, K. Ellmer, Surf. Coat. Technol. **200**, 218 (2005)
24. F. Kopnov, A. Yoffe, G. Leitus, R. Tenne, Phys. Stat. Sol. (b) **243**, 1229 (2006)
25. J.R. Ares, A. Pascual, I.J. Ferrer, C.R. Sanchez, Thin Solid Films **451**, 233 (2004)